Proceedings of the ASME 2022
International Mechanical Engineering Congress and Exposition
IMECE2022
October 30-November 3, 2022, Columbus, Ohio

IMECE2022-94871

IDENTIFICATION OF FLAWS AND ASSESSMENT OF MECHANICAL PROPERTIES IN ADDITIVELY MANUFACTURED TITANIUM PARTS USING ACOUSTIC RESONANCE ULTRASOUND SPECTROSCOPY (RUS)

Hossein Taheri
Laboratory for Advanced NonDestructive Testing, In-situ monitoring and Evaluation (LANDTIE)
Georgia Southern University
Statesboro, GA, USA

Caleb Williams
Laboratory for Advanced NonDestructive Testing, In-situ monitoring and Evaluation (LANDTIE)
Georgia Southern University
Statesboro, GA, USA

Russell Krenek
Laboratory for Advanced NonDestructive Testing, In-situ monitoring and Evaluation (LANDTIE)
Georgia Southern University
Statesboro, GA, USA

Gregory Weaver
Weaver NDT
Las Vegas, NV, USA

Mohammad Taheri
Department of Mathematics and Statistics
South Dakota State University
Brookings, SD, USA

ABSTRACT

Additive manufacturing (AM) techniques are becoming accepted as routine in many industrial fields that include aerospace applications. This ramp up in manufacturing has highlighted a fundamental need for innovative nondestructive testing (NDT) methodologies for AM inspection and qualification purposes. Resonance Ultrasound Spectroscopy (RUS) is beginning to be applied as an innovative NDT inspection technique for AM components to obtain insights from the parts' structural integrity and because it correlates to mechanical properties. RUS is used to understand sensitivity to detecting internal flaws, resulting in lower than expected failure resistance or fatigue life. Multiple test bar batches using the Ti6Al4V alloy were fabricated by powder bed fusion (PBF) AM technique at different processing conditions. RUS and destructive tests, including tensile and fatigue tests, based on ASTM standards are performed in order to evaluate the mechanical properties and tensile and fatigue strength of the parts. Finally, metallography experiments revealed the microstructure of the parts. The goal of correlation analysis is to establish the defect-NDT-property relationship for the Ti6Al4V by showing the strength and significance of the relationship between the testing data and the properties of the samples. Results show that RUS is a reliable and capable NDT technique to acquire rapid information for this purpose. This information is crucial for expanding the production and application of AM components while making sure that the mechanical properties, their structural integrity, and part safety satisfy the requirement of the lifetime operation.

Keywords: Resonant Ultrasound Spectroscopy (RUS); Additive Manufacturing (AM); Powder Bed Fusion (PBF); Tensile; Fatigue; Nondestructive Testing (NDT)

NOMENCLATURE

Place nomenclature section, if needed, here. Nomenclature should be given in a column, like this:

f_r	Resonance frequency
ρ	Density

1. INTRODUCTION

Additive manufacturing (AM) or 3D printing results in a final product being produced through addition of materials layer-by-layer to fabricate a complex geometry without using tooling and machining. A computer (CAD) model is used to generate sliced model of the part and control the layering deposition process of the material. Compared to the traditional manufacturing techniques where casting, forging, rolling, cutting, machining, and drilling is being used, additive manufacturing saves time, cost of the manufacturing, and it provides easy production of complex geometries. However, the quality inspection and testing of such complex parts are a challenging but a demanding task. Resonance Ultrasound Spectroscopy (RUS) as an innovative inspection technique for AM components. RUS will be used to understand the sensitivity to detecting internal defects, resulting in lower than expected failure resistance or fatigue life. When an object is excited, it resonates at its natural frequencies. These natural frequencies are unique to each component, but are predictable and consistent within the normal material and manufacturing tolerances. RUS capabilities are rapid testing throughput (typically less than 3 seconds per part), 100%-part coverage, automated PASS/FAIL results, and structural property correlation. This inspection will offer unique advantages for AM component production and inspection. The proposed work will include feasibility testing of RUS on actual AM test bars that will include flaws which would cause the failure of a part in service. The samples in this study will be manufactured from Titanium alloy (Ti6Al4V). This titanium alloy is widely used in aerospace and medical applications because of its superior mechanical performance. As this alloy is being used in many critical components in different industries and application, there is a crucial need to have a quick but throughout inspection technique specifically when the geometry of the part is rather complex and conventional inspections are not applicable.

RUS is a proven scientific NDT method. A properly, dimensionally and metallurgically, manufactured part that is flaw-free will produce repeatable, clean, and distinct resonances. So, a group of flaw free parts manufactured within a set of tolerances will resonate consistently within a similar tolerance range. An object that is deficient or defective will produce a variety of different resonances, which will deaden, shift, and/or dull the responses. This allows a means for a poorly repaired part or an improperly manufactured (printed) part to be verified using the distinct differences and responses. This is a proven and validated way to determine if an object is structurally sound, repeatable, and consistent.

RUS has been extensively used for quality assessment in many different industries and applications and its methodology has been developed for different sizes, geometries, defect detections and materials. Maynard explained in his article that when measuring and processing a sample's natural frequencies, one can determine the elastic constants of a broad range of crystalline and nanocrystalline materials. He has concluded that RUS is expected to become readily accessible for many research applications in near future [1]. Through measuring the elastic constants by RUS and the directional wave speeds of a polycrystalline aggregate, Lan et al. presented a method for volumetric assessment of the texture of polycrystalline materials. They extracted lower-truncation-order textures of representative hexagonal and cubic metal samples with orthorhombic sample symmetries and validated the results against independent immersion ultrasound and neutron tests [2]. In addition, as briefly mentioned above, the applicability of RUS to a wide range of sample sizes is one of the major advantages of this technique. Adebisi et al. used RUS to measure elastic properties of micrometer sized pillars of single crystals and to quantify the level of uncertainties in those measurements. Due to small sizes of samples in their study, they have developed and utilized a non-contact laser-based detection technique and showed that the level of uncertainty increases with increase in material complexities [3].

In particular, due to the promising capabilities and ease of use for more complex geometries, RUS application received significant attention for AM part qualification. Ibrahim et al. used RUS to overcome the challenge of inspecting additively manufactured lattice structures by conventional NDT techniques. They expanded their study on evaluating the suitability of RUS technique through a combined approach of experimental testing and Finite Element (FE) modeling [4]. In a similar study, McGuigan et al. used RUS experimental study along with the numerical modeling for inspection of lattice structures with a varying number of missing struts. They concluded that however pristine and defective lattices may be distinguished, the number of missing struts cannot be inferred [5]. In addition to inspection purposes, RUS has been successfully used for material characterization of additively manufactured components as well. Elastic properties of additively manufactured components can be estimated using RUS [6]–[8]. Rossin et al. demonstrated the assessment of grain structure evolution with RUS in additively manufactured nickel alloys. They showed that RUS can detect recrystallization and enables detection of texture and is extendable to other geometries, alloys and mechanisms. They have also included a FE modeling in their study for prediction of changes in resonant frequencies [9].

Material property differences, geometry variation, and defects adversely affect the structural characteristics of a part. RUS has been shown to be sensitive to material properties such as microstructure, defects and geometric deviations [10], [11]. Resonance frequency (f_r) (Eq. 1) of a part is affected by its elastic constants (C_{ijkl}), mode number (n), density (ρ) or geometrical properties ($2L$: wave propagation distance). These variables define the wavelength (λ) and wave speed (ϑ) which in turn are a function of microstructure, defect character, and most importantly for this study, the processing history of the component [12], [13].

$$f_r = \frac{\vartheta}{\lambda} = \frac{n}{2L}\sqrt{\frac{C_{ijkl}}{\rho}} \qquad (1)$$

2. MATERIALS AND METHODS

In this section the fabrication method, material, as well as experimental testing of the samples are described.

2.1 Sample Fabrication

Samples in dog-bone shape were fabricated according to ASTM E8 [14]. The cross-section area of the samples in gauge-length area was 6x6 mm. Powder Bed Fusion (PBF) AM method was used to manufacture samples from Ti6Al4V alloy powders. Samples were fabricated at 3 different process parameters including: (1) Optimized process (Group A), (2) Decrease the input energy density to generate potential lack-of-fusion flaws (Group B), (3) Decrease the printing speed which cause an increased rate of cooling to generate potential thermal stress and/or hot-cracking flaws (Group C). Five (5) samples were made at each processing condition making the total number of samples to be fifteen (15) samples.

2.2 RUS Experimental Setup

A schematic and photo of the RUS test setup is shown in Figure 1. The experimental tests were conducted by Weaver NDT using an NDT-RAM Resonant Ultrasound Spectrometer system by Modal Shop [15]. The samples were excited, and the resonance data of each part was collected twice to investigate the repeatability of the measurements. Each part was impacted by gently tapping the part on the modal hammer. The measured spectra are first globally normalized to have a unit maximum amplitude. Figure 2 shows a typical data captured and recorded by the NDT-RAM equipment and software.

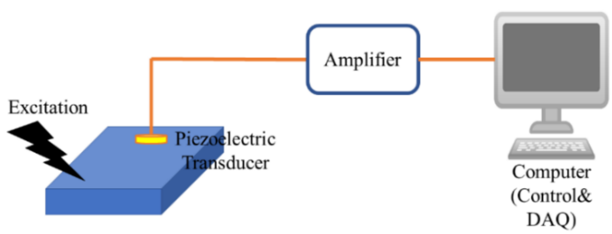

(A)

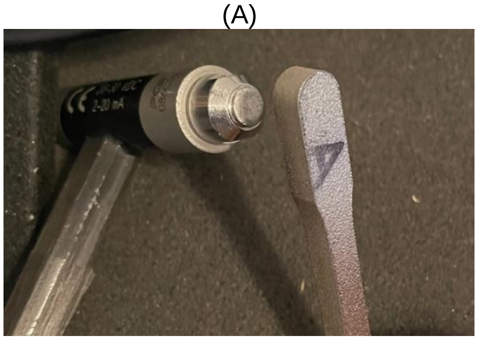

(B)

FIGURE 1: EXPERIEMNTAL SETUP FOR RESONANCE ULTRASOUND SPECTROSCOPY (RUS)

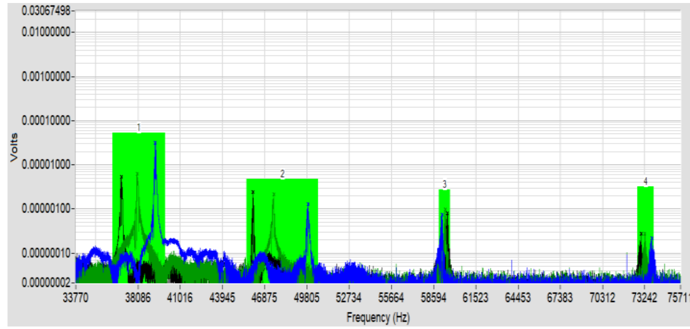

FIGURE 2: TYPICAL DATA CAPTURED AND RECORDED BY THE NDT-RAM EQUIPMENT AND SOFTWARE

Each the samples were tested twice by RUS and data were recorded for post processing.

2.3 Fatigue and Tensile Tests

Fatigue and tensile testing were done on samples to acquire mechanical properties of the samples such as tensile strength, ultimate strength and fatigue strength. Tensile tests were performed by an Instron universal testing machine at the rate of 1.75 mm/min until failure happened. Fatigue tests were completed at stress amplitude of 395 MPa, R=0.1 and 10 Hz frequency until the failure occurred.

2.4 Metallography

To study the flaw formation such as porosity in the samples at different process conditions, samples were sectioned on the cross-section area, mounted and polished for microscopy imaging. Optical microscopy imaging at 10x magnification was completed on all samples.

2.5 Nanoindentation

Nanoindentation technique is used to measure the mechanical properties of materials, specifically hardness (H) and modulus of elasticity (E), with high precision. These properties are estimated from the load (P) versus displacement (h) measurement data recorded during the test [16]. Figure 3 shows the NHT2 nanoindenter (Anton Paar, USA) and sample setup in the instrument.

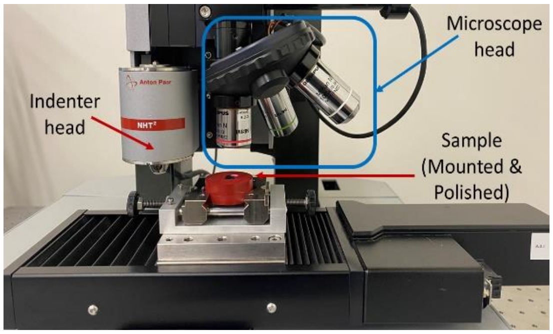

(A)

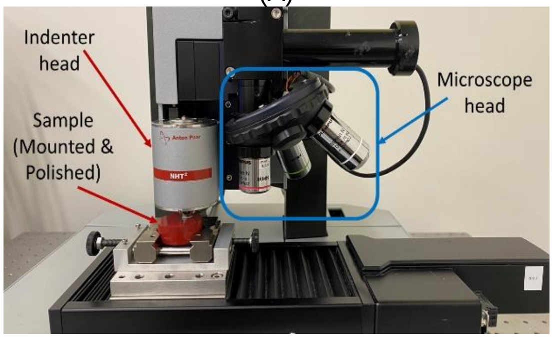

(B)

FIGURE 3: NANOINDENTER INSTRUMENT AND SAMPLE SETUP UNDER THE (A) MICROSCOPE HEAD OF THE INSTRUMENT, AND (B) INDENTER HEAD OF INSTRUMENT

3. RESULTS AND DISCUSSION

All testing results were recorded, gathered and analyzed for each group of samples made at the different processing conditions. This section provides a summary of the testing results.

3.1 RUS Testing

Figure 4 shows the entire usable frequency spectrum of the RUS testing on the samples, with the frequency on the horizontal axis and the amplitude on the vertical axis. Each of the separate colors are the individual A, B, and C groups of samples. The green color boxes show a selected criteria band for each frequency. These bands are setup based on the distribution of each individual frequency response. The all the parts were used to set the boundaries. Frequency spectrum of the RUS testing presented in Figure 4 shows that there is a clear change in both the resonance frequency and the amplitude of the spectrum for each group of the samples. These changes in resonance frequency spectrum are the indications of the variation in material properties and structural integrity in different groups of samples which are caused by variation on process parameters.

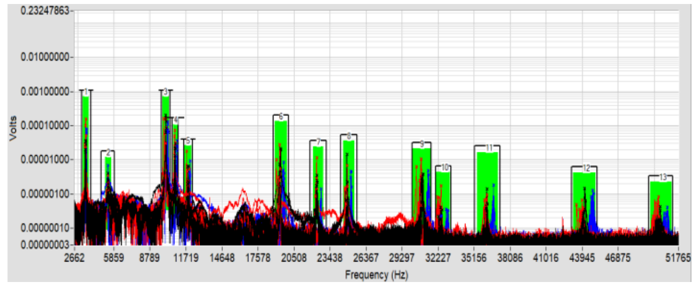

FIGURE 4: USABLE FREQUENCY SPECTRUM OF ALL THE PARTS

The RUS raw frequency data can be exported into a report format and that data can be used in many ways for analysis. For samples in this study that are to be subjected to some type of destructive testing, the individual frequencies absolute responses should be evaluated for trending that correlates to the mechanical property results. In addition to the absolute frequency response, another statistic option to understanding frequency correlation to structural properties is a Z-score analysis.

Z-score is a measure of a part's location within a population, relative to the population mean, in units of the population standard deviation. A part that falls 3 standard deviations below the mean will have a Z-score of -3. The variation in the Z score represents the similarity of the resonance pattern of a specific part to the population's patterns. Parts that vary in a different manner have higher Z-score variation. The Z-score measurement is an excellent way to understand a population of parts. It can be used to find Outlier parts or to understand if processes are drifting over time, batch to batch, or build to build. The Z-score analysis of these samples is shown in Figure 5. From the Z-score plot in Figure 5, the samples in group A have clearly an isolated cluster of response compared to group B and C which are manufactured with deviation from the optimum manufacturing process conditions.

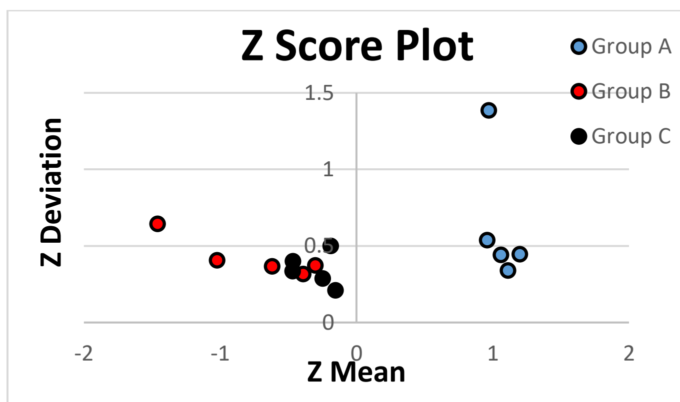

FIGURE 5: Z-SCORE PLOT OF THE SAMPLES FOR GROUP A, B AND C

3.2 Tensile Testing

Figure 6 shows the stress-strain curves for the average values of the tensile test results for each group of samples. Table

1 shows the average values for yield, tensile and elongation for each group of samples.

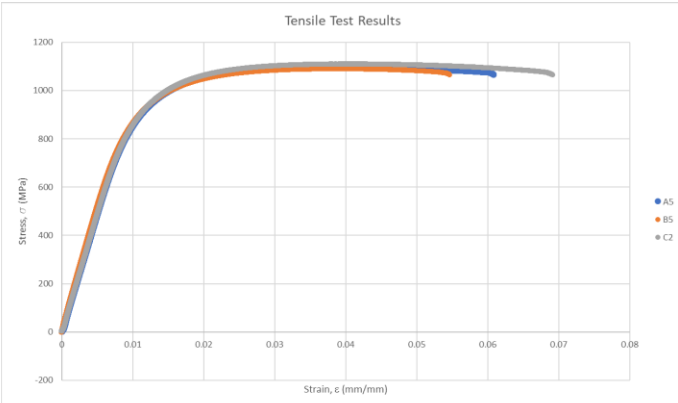

FIGURE 6: STRESS-STRAIN CURVES FOR THE AVERAGE VALUES OF THE TENSILE TEST RESULTS FOR EACH GROUP OF SAMPLES

TABLE 1: AVERAGE VALUES FOR YIELD, TENSILE AND ELONGATION FOR EACH GROUP OF SAMPLES

Group	Yield (MPa)	Tensile (MPa)	Elongation (mm/mm)
A	886	1096	0.06082
B	864	1089	0.05448
C	880	1065	0.06904

From the tensile test results, the samples manufactured in optimum processing condition show a slightly higher yield and tensile strength as expected, but the difference is not very significant. In addition, the elongation in group C of the samples was the highest number between groups which needs to be investigated through additional assessments.

3.3 Fatigue Testing

Figure 5 shows the stress range evolution at constant stress amplitude results for each group of samples. The average number of cycles to failure for group A was 3486, group B was 2115 and group C was 2820. Despite the small changes which have been seen in tensile testing results, a higher level of variation can be seen in the fatigue properties of the samples manufactured in different process conditions. Samples in group A, manufactured with optimum process condition, showed a considerably higher number of cycles until the failure and at a much lower strain range compared to samples in groups B and C. The variation in manufacturing processing conditions applied for groups B and C changed the material properties and structural integrity of the samples and potentially generated some defects in those samples such as porosities and micro-cracking which could influence the fatigue behavior of the parts as described in many other investigations [17], [18].

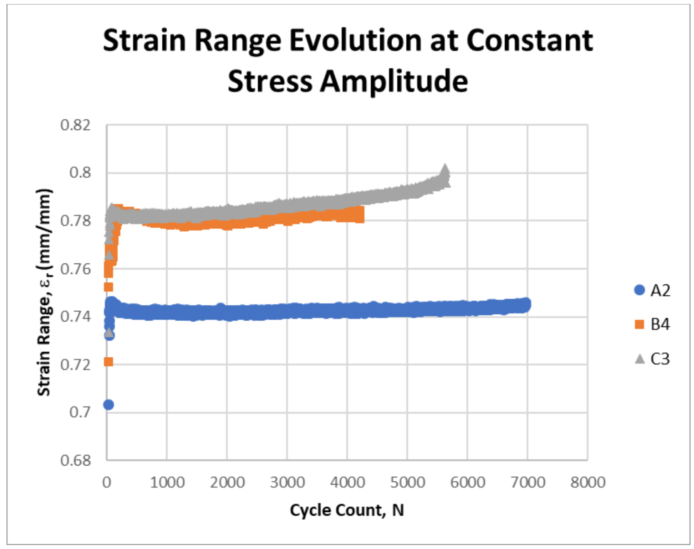

FIGURE 6: STRESS RANGE EVOLUTION AT CONSTANT STRESS AMPLITUDE RESULTS FOR EACH GROUP OF SAMPLES

3.3 Metallography Testing

Metallography of the internal structure of the samples using optical microscopy is a common and useful technique for visualization of the internal structure as well as topography and shapes of potential defects in the parts. Figure 7 shows the cross-section microscopy imaging results for each group of samples. Samples were first sectioned to an appropriate size in their cross-section view and mounted into a traditional polymer mounting powders for metallography. Then, they were polished at three different grades of polishing pads until a mirror-like surface is acquired suitable for visualization and microscopy.

GROUP A

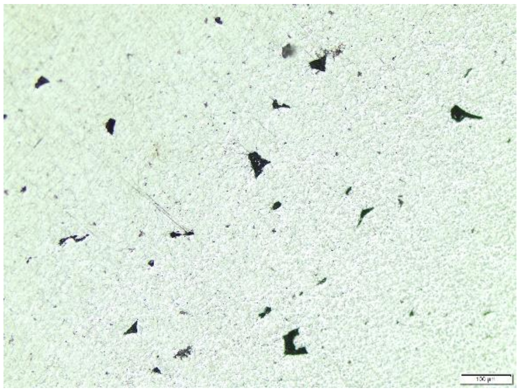

GROUP B

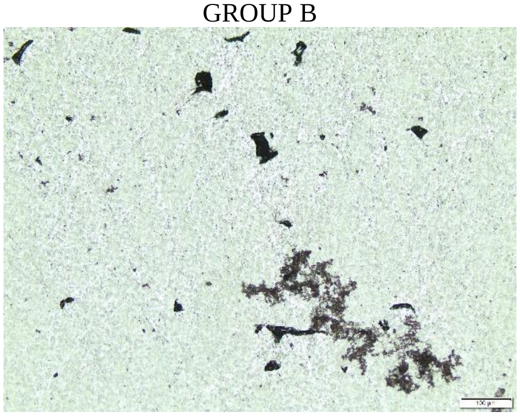

GROUP C

FIGURE 7: CROSS-SECTION MICROSCOPY IMAGING RESULTS FOR EACH GROUP OF SAMPLES

The microscopy imaging results in Figure 7 shows a clear difference in flaw and porosity generation, as well as level and size of flaw differences in each group of samples.

3.4 Nanoindentation Testing

Nanoindentation tests were done over the mounted and polished cross section of the samples A, B and C at total of 25 points distributed in a 5x5 grid where the distance between each grid point (indentation test location) was 1 mm. This matrix of recorded data helps to find a more robust average of the measurements, as well as investigating if there is any significant variation of measurement over the cross-section area of each sample which would be an indicator of inhomogeneity within a sample. Figure 8 shows one of the indentation points for sample A and the average values of the hardness (H) and modulus of elasticity (E) for all samples.

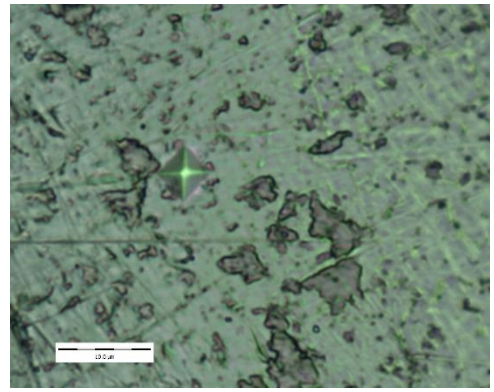

(A)

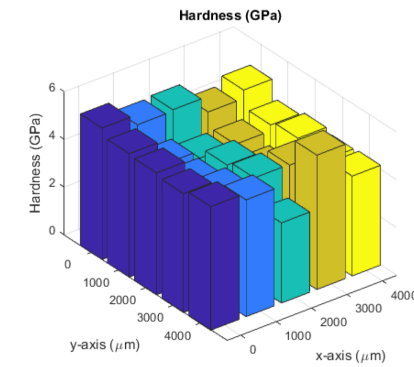

(B)

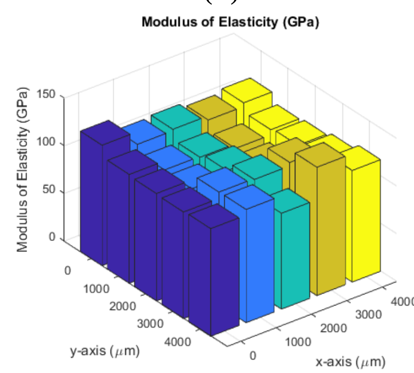

(C)

FIGURE 8: (A) IMAGE OF AN INDENTATION POINTS FOR SAMPLE C, AND (B) THE VALUES OF THE HARDNESS (H) AND (C) THE VALUES OF MODULUS OF ELASTICITY (E) FOR ALL INDENTATION POINTS OVER THE SPECIFIED 5x5 GRID

4. CONCLUSION

An experimental study for assessment of correlation between the resonance ultrasound spectroscopy and structural integrity and mechanical properties of the additively manufactured Titanium samples fabricated by powder bed fusion techniques was presented. Results show clear differences between the RUS natural frequency responses as well as mechanical property testing for each of the groups of the samples. This study makes clear that RUS results can be correlated to flaw presence, mechanical property testing, and the overall structural integrity of the samples. RUS is a rapid indicator of the parts quality.

ACKNOWLEDGEMENTS

Authors acknowledge Georgia Southern University's Faculty Research Committee and American Society for Nondestructive Testing (ASNT) for the support of this work through 2021 Faculty Research Award and 2022 ASNT Fellowship Award. Authors also thank all of the LANDTIE's collaborators who have helped with different part of this work from sample manufacturing (Quad City Manufacturing Laboratory) to testing and experiments (WeaverNDT, Pinnacle Industrial X-Ray Laboratory, and Georgia Tech Research Corporation ("GTRC")).

REFERENCES

[1] J. Maynard, "Resonant ultrasound spectroscopy," *Phys. Today*, vol. 49, no. 1, pp. 26–31, 1996, doi: 10.1063/1.881483.

[2] B. Lan, M. A. Carpenter, W. Gan, M. Hofmann, F. P. E. Dunne, and M. J. S. Lowe, "Rapid measurement of volumetric texture using resonant ultrasound spectroscopy," *Scr. Mater.*, vol. 157, pp. 44–48, 2018, doi: 10.1016/j.scriptamat.2018.07.029.

[3] R. A. Adebisi, T. J. Lesthaeghe, M. R. Cherry, S. Sathish, and P. A. Shade, "Development of a LASER-based resonant ultrasound spectroscopy and a framework for error propagation in the estimated elastic moduli," *AIP Conf. Proc.*, vol. 1949, 2018, doi: 10.1063/1.5031626.

[4] Y. Ibrahim, Z. Li, C. M. Davies, C. Maharaj, J. P. Dear, and P. A. Hooper, "Acoustic resonance testing of additive manufactured lattice structures," *Addit. Manuf.*, vol. 24, no. July, pp. 566–576, 2018, doi: 10.1016/j.addma.2018.10.034.

[5] S. McGuigan, A. P. Arguelles, A. F. Obaton, A. M. Donmez, J. Riviere, and P. Shokouhi, "Resonant ultrasound spectroscopy for quality control of geometrically complex additively manufactured components," *Addit. Manuf.*, vol. 39, no. September 2020, p. 101808, 2021, doi: 10.1016/j.addma.2020.101808.

[6] K. A. Fisher, "Estimation of elastic properties of an additively manufactured lattice using resonant ultrasound spectroscopy," *J. Acoust. Soc. Am.*, vol. 148, no. 6, pp. 4025–4036, Dec. 2020, doi: 10.1121/10.0002964.

[7] B. Maiorov, "Determining the full elastic tensor using resonant ultrasound spectroscopy in extreme environments," *J. Acoust. Soc. Am.*, vol. 149, no. 4, pp. A125–A125, Apr. 2021, doi: 10.1121/10.0004736.

[8] A. Karunarathne *et al.*, "Resonant ultrasound spectroscopy measurement of elastic properties of SnSe," *J. Acoust. Soc. Am.*, vol. 142, no. 4, p. 2575, Oct. 2017, doi: 10.1121/1.5014413.

[9] J. Rossin *et al.*, "Assessment of grain structure evolution with resonant ultrasound spectroscopy in additively manufactured nickel alloys," *Mater. Charact.*, vol. 167, p. 110501, 2020, doi: 10.1016/j.matchar.2020.110501.

[10] B. Kianian, "Wohlers Report 2017: 3D Printing and Additive Manufacturing State of the Industry, Annual Worldwide Progress Report," Fort Collins, Colorado, 2017.

[11] H. Taheri, F. Dababneh, G. Weaver, and B. Butsch, "Assessment of material property variations with resonant ultrasound spectroscopy (RUS) when using additive manufacturing to print over existing parts," *J. Adv. Join. Process.*, vol. 5, p. 100117, 2022, doi: 10.1016/j.jajp.2022.100117.

[12] G. Tapia, A. H. Elwany, and H. Sang, "Prediction of porosity in metal-based additive manufacturing using spatial Gaussian process models," *Addit. Manuf.*, vol. 12, pp. 282–290, 2016, doi: 10.1016/j.addma.2016.05.009.

[13] P. C. Collins, D. A. Brice, P. Samimi, I. Ghamarian, and H. L. Fraser, "Microstructural Control of Additively Manufactured Metallic Materials," *Annu. Rev. Mater. Res.*, vol. 46, pp. 63–91, 2016, doi: 10.1146/annurev-matsci-070115-031816.

[14] ASTM Int., "Standard Test Methods for Tension Testing of Metallic Materials - E8/E8M," *ASTM*, no. C, pp. 1–27, 2009, doi: 10.1520/E0008.

[15] "The Modal Shop." https://www.modalshop.com/.

[16] M. S. Hossain, M. Baniasadi, and H. Taheri, "Material characterisation of additive manufacturing titanium alloy (Titanium 6Al-4V) for quality control and properties evaluations," *Adv. Mater. Process. Technol.*, pp. 1–20, Jun. 2022, doi: 10.1080/2374068X.2022.2079589.

[17] R. Esmaeilizadeh *et al.*, "On the effect of laser powder-bed fusion process parameters on quasi-static and fatigue behaviour of Hastelloy X: A microstructure/defect interaction study," *Addit. Manuf.*, vol. 38, p. 101805, 2021.

[18] A. Kaletsch, S. Qin, S. Herzog, and C. Broeckmann, "Influence of high initial porosity introduced by laser powder bed fusion on the fatigue strength of Inconel 718 after post-processing with hot isostatic pressing," *Addit. Manuf.*, vol. 47, p. 102331, 2021.